

# SILICON PHOTONIC DISSOLVED CO<sub>2</sub> SENSING SYSTEM FOR PERFLUOROCARBON-BASED PERITONEAL OXYGENATION

Bibek Ramdam<sup>1</sup>, Hyun-Tae Kim<sup>1</sup>, Behzad Kadkhodaeielyaderani<sup>1</sup>, Yejin Moon<sup>1</sup>, Parham Rezaei<sup>1</sup>, Melissa J. Culligan<sup>2</sup>, Nosayaba Enofe<sup>1</sup>, Dawn Forste<sup>2</sup>, Alexis Freiling<sup>2</sup>, Karen Davalos<sup>2</sup>, Maria Altemos<sup>3</sup>, Josphah Friedberg<sup>2</sup>, Hosam K. Fathy<sup>1</sup>, Jin-Oh Hahn<sup>1</sup>, and Miao Yu<sup>1</sup>

<sup>1</sup>University of Maryland, USA,

<sup>2</sup>Temple University, USA, and

<sup>3</sup>Thomas Jefferson University, USA

## ABSTRACT

This paper reports a silicon photonic dissolved CO<sub>2</sub> sensing system, which, for the first time, allows monitoring of extra-pulmonary gas exchange during peritoneal oxygenation with perfluorocarbon (PFC). This work highlights the transition of the photonic sensor from controlled laboratory setups to an operating room by using a compact and cost-effective optical interrogator. In swine experiments, 4% CO<sub>2</sub> dissolved in the PFC circulating in the animal's peritoneal cavity is measured demonstrating the sensing system's potential for real-world biomedical gas monitoring applications beyond just this one.

## KEYWORDS

Silicon Photonics, Ring Resonators, Peritoneal Perfusion, Perfluorocarbon Perfusion, Dissolved CO<sub>2</sub> Sensor, Biomedical Gas Sensor

## INTRODUCTION

Although mechanical ventilation is widely used for patients with respiratory failure, including those with moderate to severe COVID-19 infection, it often leads to ventilator-induced lung injury (VILI) [1]. To mitigate VILI, significant research has been done towards novel extrapulmonary gas exchange techniques such as peritoneal

oxygenation, where oxygen is delivered into the peritoneal cavity via carriers like PFCs that possess extraordinary O<sub>2</sub> and CO<sub>2</sub> solubility [2]. However, there is a lack of sensors capable of detecting dissolved gases in PFCs, as most commercial dissolved gas sensors operate only in aqueous solutions. Recently, a silicon photonic sensor capable of detecting dissolved CO<sub>2</sub> in PFC was proposed by our group [3]. Silicon photonics platform comes with several advantages of the already mature complementary metal-oxide-semiconductor (CMOS) process such as high yields from a robust fabrication method at a relatively low cost [4]. Additionally, ring resonators make use of optical waveguides with reduced footprint, enabling device miniaturization [5]. When gas molecules interact with an optical waveguide, they alter the surrounding refractive index (RI), leading to a significant change in the optical transmission [6]. One of the limitations of the RI-based sensing was the lack of selectivity to a specific gas. However, recent advancements of metal organic frameworks (MOFs), a class of crystalline materials with tunable porosity and adjustable internal surface properties, have made it possible to find materials that are sensitive to specific target gas [7]. One particular MOF that has been extensively studied for RI-based sensing of CO<sub>2</sub> is Zeolitic Imidazolate Framework 8 (ZIF-8) [3], [8], [9]. Despite this advancement, challenges remain in transitioning the

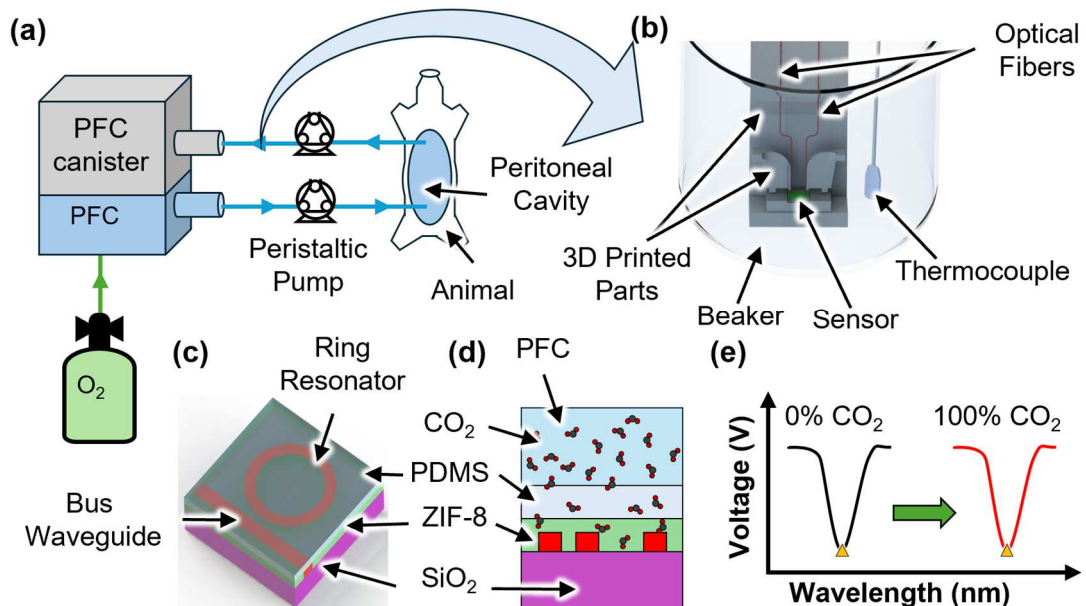


Figure 1: (a) Simplified flow configuration for pumping oxygenated PFC into the animal's peritoneal cavity and collecting the returning PFC. (b) PFC returning from the animal is sampled out into a beaker to measure the dissolved CO<sub>2</sub>. (c) Schematic of the sensor showing the ring and bus waveguides. (d) Cross-section of the sensor with different layers of materials used. (e) Schematic of resonant dip experiencing a redshift in the presence of CO<sub>2</sub>.

photonic sensor from a controlled laboratory setup to an operating room or other clinical settings for practical applications due to the bulky and expensive interrogation and signal processing equipment [10].

In this paper, we demonstrate a photonic sensor capable of measuring the dissolved  $\text{CO}_2$  in the PFC being perfused into the peritoneal cavity of a swine. The goal of peritoneal perfusion of oxygenated PFCs is two folds: (i) animal oxygenation during hypoxia and (ii) simultaneous  $\text{CO}_2$  removal during hypercarbia. During the perfusion experiment, the animal is subjected to hypoxia, a condition characterized by reduced oxygen delivery to the body's tissue. Our team has already tried to estimate the rate at which perfusion removes  $\text{CO}_2$  in [11], but this new sensor allows us to actually measure this rate, for the first time. Additionally, to the best of our knowledge, this is the first of its kind report that demonstrates a photonic microring resonator-based sensor and its interrogation system to understand the gas exchanges happening during peritoneal PFC perfusion.

## EXPERIMENTAL SETUP

A compact and cost-effective photonic dissolved  $\text{CO}_2$  sensing system has been developed using a Fabry-Perot (FP) tunable filter-based interrogator, allowing the measurement of dissolved  $\text{CO}_2$  in PFC during the peritoneal oxygenation of swine. Figure 1(a) shows a simplified version of the peritoneal perfusion system used by researchers in [12], where PFC is both oxygenated and heated to 39°C in a large canister. Then, a couple of peristaltic pumps are used for PFC perfusion into and out of the animal's peritoneal cavity. Once the animal has been subjected to hypoxia, induced by reducing the fraction of inspired oxygen ( $\text{FIO}_2$ ) for approximately 20 minutes, a small amount of PFC returning to the canister is sampled out and poured into a glass beaker containing the silicon photonics based dissolved  $\text{CO}_2$  sensor. Figure 1(b) shows the aforementioned sensor in addition to a thermocouple for continuous temperature measurement. Although it is not illustrated in Figure 1 (b), the entire beaker was placed on top of a hot plate to maintain the environment inside the beaker to be close to the PFC circulating in the animal. Additionally, the beaker setup was also covered with aluminum foil to maintain a somewhat enclosed environment for the testing. Transportation of sampled PFC to sensor beaker took less than 20 seconds. Figure 1(c) illustrates the schematic of the silicon ring resonator-based  $\text{CO}_2$  sensor that was fabricated using the well-established CMOS process, details of which can be found in [3]. Figure 1(d) shows the cross-section of the sensor coated with ZIF-8, a metal organic framework (MOF) that enables selective and sensitive  $\text{CO}_2$  detection, and a protective barrier layer of PDMS that protects ZIF-8 from biofluids. Exposure to  $\text{CO}_2$  induces a redshift in the resonance wavelength, that corresponds with the gas concentration, as depicted in Figure 1(e), enabling the measurement of dissolved  $\text{CO}_2$ .

The optical setup for sensor interrogation is illustrated in Figure 2. Broadband light is coupled into an FP tunable filter to obtain a narrow linewidth scanning light. The scanning light is split into the sensing and reference arms in ratios of 99:1 using a coupler. The sensing arm directs light to the sensor, whereas the reference arm uses three

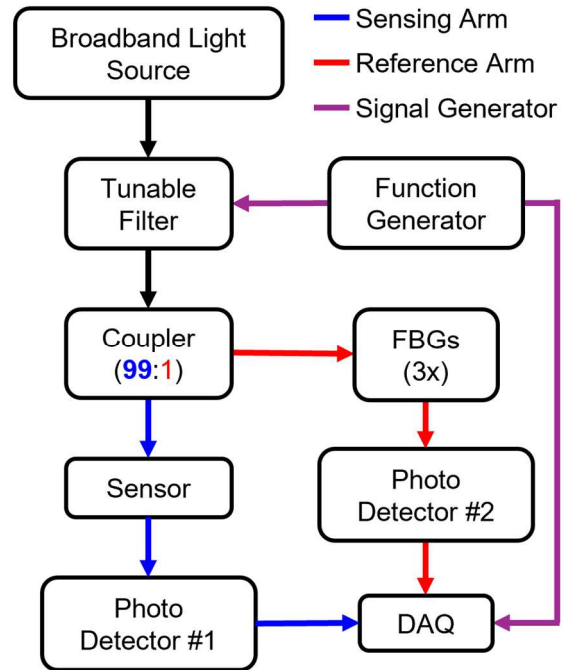


Figure 2: Sensor interrogation setup. Broadband light is filtered into a narrow band by a tunable filter driven by a function generator. Light is then split by a coupler. 99% of the light is passed to the sensing arm and remaining 1% is passed to the reference arm.

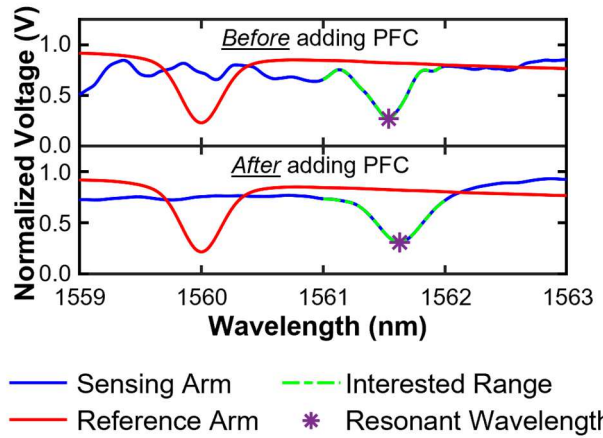


Figure 3: Signal processing method to extract resonant wavelength. The wavelength profile changes when the sensor comes in contact with PFC containing  $\text{CO}_2$ , whereas the reference arm's profile (obtained from the FBGs) remains the same. The sensor's resonant wavelength (purple \*) is then tracked within the range of interest. The resonance dip at 1560 nm in the reference arm corresponds to one of the FBGs. Note that the other two FBGs have not been shown.

fiber Bragg gratings (FBGs) for wavelength calibration of the scanning light. Signal from each arm is collected via photoreceiver. A function generator drives the scanning wavelength of the tunable filter back and forth by using a triangular waveform with a frequency of 0.1 Hz. The data from the sensing arm, reference arm, thermocouple, and the function generator's waveform are recorded in the temporal domain using a data acquisition (DAQ) system.

## RESULTS AND DISCUSSIONS

The data from the DAQ, which is recorded with reference to time, is converted into wavelength information using the three reference FBGs for every cycle of the function generator's triangular waveform. The Bragg wavelengths of the FBGs remain relatively stable because they were kept isolated and secure throughout the experiment. Figure 3 shows the transmission spectra obtained from the reference and sensing arms once the time domain has been converted into wavelength domain. The reference FBG of 1560 nm is shown by the red curve, and the sensor's response is shown by the blue curve. The green region between 1561-1562 nm within the blue curve is the region of interest where we are tracking the resonance dip of the sensor. The resonance dip is shown by the purple asterisk. The plots on top and bottom showcases just before and after pouring PFC from the animal. Comparing the top and bottom plots, it is clear that the resonant wavelength shifts to the right when PFC containing dissolved  $\text{CO}_2$  comes in contact with the sensor. It should be noted that the resonance dip is tracked for every cycle of the function generator's triangular waveform that drives the tunable filter. Therefore, a resonant dip is obtained once every 10 seconds for a given test.

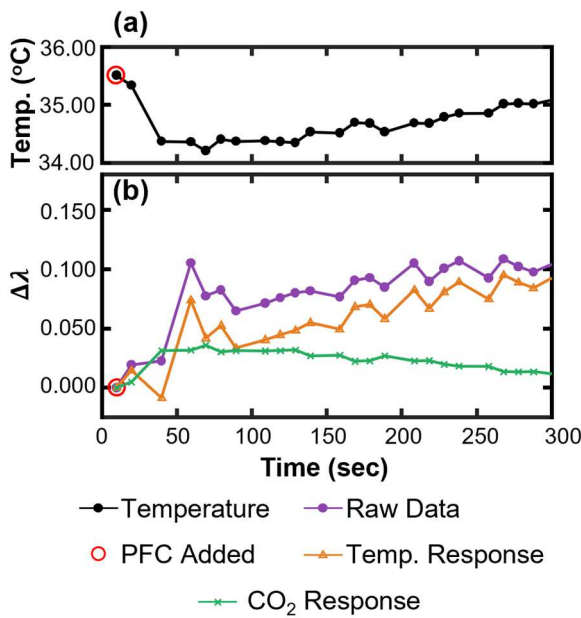


Figure 4: (a) Representative temperature measured inside the beaker by using the thermocouple. (b) Sensor responses in terms of wavelength shifts. The raw data is the response to both the  $\text{CO}_2$  level and the temperature. The orange curve shows the response to temperature only. The green curve shows the response to  $\text{CO}_2$  after temperature compensation.

The results obtained after measuring the dissolved  $\text{CO}_2$  in the sampled-out PFC after one of the 20-min-long hypoxia experiments are shown in Figure 4. The temperature data recorded using the thermocouple placed alongside the sensor is shown in Figure 4(a). The point where PFC is added into the sensor beaker is indicated by a red circle. There is a sharp decrease in the temperature as PFC from the animal is added into the beaker. This is because the beaker's internal temperature is higher than the PFC coming out of the animal. Similarly, there is a gradual increase in the temperature with time because the PFC gets

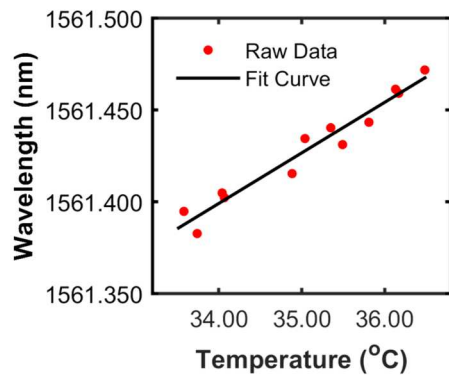


Figure 5: Temperature sensitivity calibration curve obtained by plotting the resonant wavelength as a function of temperature measured by a thermocouple.

heated as the entire beaker is still on top of a hot plate. Figure 4(b) shows the response from the sensor where the raw data is indicated by a purple curve. This purple curve reflects both temperature and  $\text{CO}_2$  effects. To isolate the  $\text{CO}_2$  response, the temperature-induced wavelength shift ( $\lambda_\theta$ ) (orange curve in Figure 4(b)) of the resonant wavelength is calculated using the equation  $\lambda_\theta = \lambda_n + S_\theta \cdot (\theta_n - \theta_i)$ . Here,  $S_\theta$  is the temperature sensitivity obtained from Figure 5, which shows the resonant wavelength shift vs. temperature, and is found to be 0.0276 nm/°C. Likewise,  $\lambda_n$  and  $\theta_n$  represents wavelengths and temperatures at any given time, respectively. Similarly,  $\theta_i$  is the temperature when PFC was added. Subtracting  $\lambda_\theta$  from the raw data gives the  $\text{CO}_2$  response, shown as the green curve in Figure 4(b).

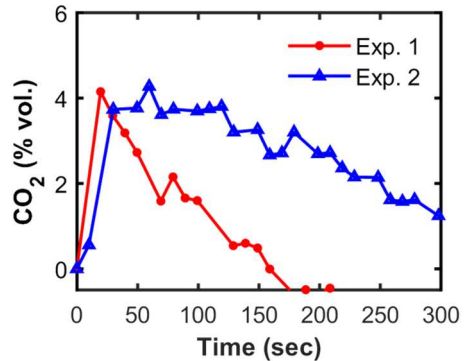


Figure 6:  $\text{CO}_2$  response obtained from two experimental trials at the end of two 20-min-long hypoxia trials. Note there is a 5-min-long recovery time between the two experiments.

The obtained resonance shifts are converted to dissolved  $\text{CO}_2$  levels based on the sensor's  $\text{CO}_2$  sensitivity of 0.0084 nm/% vol  $\text{CO}_2$  obtained using a similar experiment as described in [3]. Results from two experiments show a steep rise to 4%  $\text{CO}_2$  during the first ~30 seconds, followed by a gradual decrease corresponding to outgassing over time (Figure 6). This trend agrees well with the results obtained in the controlled laboratory conditions [3].

## CONCLUSION

In this paper, we demonstrated the in-field deployment of a silicon photonic dissolved  $\text{CO}_2$  sensor integrated with its interrogation system for monitoring of extra-pulmonary

gas exchange taking place during peritoneal oxygenation of a swine with perfluorocarbon (PFC). This work elevates the photonic sensor from limitations imposed by a controlled laboratory test setup with its expensive and bulky equipment to being deployed in an operating room or clinical setup using cost-effective and portable optical interrogation system. Similarly, 4-6% of CO<sub>2</sub> dissolved was measured giving credence to the assumption that gas exchange is happening between the perfused oxygen-rich PFC and the body tissues. While peritoneal oxygenation is the motivating application for this work, the potential value of a sensor capable of measuring dissolved CO<sub>2</sub> in PFC extends far beyond just this one application. For future work, the photonic sensor can be designed to have an integrated temperature monitoring ring to better compensate for temperature effects. Furthermore, the sensor can be mounted to the PFC circulation system for continuous monitoring of the dissolved CO<sub>2</sub>.

## ACKNOWLEDGEMENTS

This work was supported by the National Science Foundation (USA) Growing Convergence Research (GCR) program (2121110 and 2227939). Additionally, the researchers would like to thank the staff of the FabLab at University of Maryland for allowing us to use their facilities.

## REFERENCES

- [1] S. Sood, H. A. Ganatra, F. Perez Marques, and T. R. Langner, “Complications during mechanical ventilation—A pediatric intensive care perspective,” *Front. Med.*, vol. 10, Feb. 2023, doi: 10.3389/fmed.2023.1016316.
- [2] J. L. Leibowitz *et al.*, “320 Oxygenated Peritoneal Perfluorodecalin Improves Response to Normobaric Hypoxic Exposure in Swine,” *J. Clin. Transl. Sci.*, vol. 7, no. s1, pp. 96–96, Apr. 2023, doi: 10.1017/cts.2023.371.
- [3] H.-T. Kim, B. Ramdam, and M. Yu, “Silicon ring resonator with ZIF-8/PDMS cladding for sensing dissolved CO<sub>2</sub> gas in perfluorocarbon solutions,” *Sens. Actuators B Chem.*, vol. 404, p. 135305, 2024.
- [4] S. Y. Siew *et al.*, “Review of Silicon Photonics Technology and Platform Development,” *J. Light. Technol.*, vol. 39, no. 13, pp. 4374–4389, Jul. 2021.
- [5] W. Bogaerts *et al.*, “Silicon microring resonators,” *Laser Photonics Rev.*, vol. 6, no. 1, pp. 47–73, 2012, doi: 10.1002/lpor.201100017.
- [6] T. Claes, W. Bogaerts, and P. Bienstman, “Experimental characterization of a silicon photonic biosensor consisting of two cascaded ring resonators based on the Vernier-effect and introduction of a curve fitting method for an improved detection limit,” *Opt. Express*, vol. 18, no. 22, pp. 22747–22761, Oct. 2010, doi: 10.1364/OE.18.022747.
- [7] “Introduction to Metal–Organic Frameworks,” *Chem. Rev.*, vol. 112, no. 2, pp. 673–674, Feb. 2012, doi: 10.1021/cr300014x.
- [8] H.-T. Kim, W. Hwang, Y. Liu, and M. Yu, “Ultracompact gas sensor with metal-organic-framework-based differential fiber-optic Fabry-Perot nanocavities,” *Opt. Express*, vol. 28, no. 20, pp. 29937–29947, Sep. 2020, doi: 10.1364/OE.396146.
- [9] B. Chocarro-Ruiz *et al.*, “A CO<sub>2</sub> optical sensor based on self-assembled metal–organic framework nanoparticles,” *J. Mater. Chem. A*, vol. 6, no. 27, pp. 13171–13177, Jul. 2018, doi: 10.1039/C8TA02767F.
- [10] G. Ramírez-García, L. Wang, A. K. Yetisen, and E. Morales-Narváez, “Photonic Solutions for Challenges in Sensing,” *ACS Omega*, vol. 9, no. 24, pp. 25415–25420, Jun. 2024, doi: 10.1021/acsomega.4c01953.
- [11] M. Doosthosseini *et al.*, “Estimating the Impact of Peritoneal Perfluorocarbon Perfusion on Carbon Dioxide Transport Dynamics in a Laboratory Animal,” in *2022 American Control Conference (ACC)*, Jun. 2022, pp. 3000–3005. doi: 10.23919/ACC53348.2022.9867437.
- [12] Y. Moon *et al.*, “Safe Model-Based Multivariable Control of Peritoneal Perfusion,” *IFAC-Pap.*, vol. 56, no. 3, pp. 301–306, Jan. 2023, doi: 10.1016/j.ifacol.2023.12.041.

## CONTACT

\*Miao Yu, tel: +1-301-405-3591; [mmyu@umd.edu](mailto:mmyu@umd.edu)